



Voltage Control Strategy for Direct-drive Robots Driven by Permanent Magnet Synchronous Motors

M. M. Fateh*, M. Sadeghijaleh

Department of Electrical and Robotic Engineering, Shahrood University of Technology, Iran

PAPER INFO

Paper history:

Received 15 August 2014
Received in revised form 11 October 2014
Accepted in 18 December 2014

Keywords:

Direct-Drive Robot
Permanent Magnet Synchronous Motor
Torque Control Strategy
Voltage Control Strategy

ABSTRACT

Torque control strategy is a common strategy to control robotic manipulators. However, it becomes complex due to manipulator dynamics. In addition, position control of permanent magnet synchronous motors (PMSMs) is a complicated control. Therefore, tracking control of robots driven by PMSMs is a challenging problem. This article presents a novel tracking control of electrically driven robots which is simple and free from manipulator model. The novelty is the developing of voltage control strategy for the direct-drive robots driven by PMSMs. In addition, a state-space model is obtained for the robotic system including the direct-drive robot manipulator and the PMSMs. Then, the proposed approach is verified by stability analysis. A comparative study through simulations shows the superiority of the voltage control strategy to the torque control strategy.

doi: 10.5829/idosi.ije.2015.28.05b.09

1. INTRODUCTION

Permanent Magnet Synchronous Motors are receiving increased attention in the recent years because of their high efficiency, large torque to volume ratio, and reliable operation [1]. The controllability of PMSMs is one of the most favorite features in the control applications. PMSMs play an important role in motion control applications such as robotics and machine tool drives from a low to medium power ranges [2]. PMSMs can be used for drive-drive robot manipulators to perform high-accuracy and high-speed applications.

So far, some control strategies namely the open-loop volts/hertz control, field oriented control (FOC) [3, 4] and direct torque control (DTC) [5-7] have been introduced for speed regulation of PMSMs. Among them, the open-loop volts/hertz control yields a poor torque regulation with a slow dynamic performance and significant limitations such as the deficient torque development at low speed [8]. FOC achieves a fast response with smooth starting and acceleration [2].

However, accurate information requires the motor parameters and load conditions to guarantee good drive performance in terms of precision, bandwidth and disturbance rejection [8]. The DTC possesses several advantages over the FOC such as the elimination of coordinate transformation, lesser parameter dependence, faster dynamic response [9], and torque and flux are regulated directly and independently [10]. Nevertheless, the inability to accurately estimate the stator flux at low speeds is its main drawback [1]. So far, control of robot manipulators is based on the torque control strategy (TCS). Torque control strategy is a common strategy to control robot manipulators. The position control of robot manipulator is implemented using a torque control law. In this strategy, the dynamics of motors are excluded from the control problem. It is assumed that the motors are able to perfectly generate the control law. Then, the commonly used strategies such as the DTC or the FOC may be used to drive the PMSMs of direct-drive robot manipulators. There would seem to be some major shortcomings in the TCS. This strategy excludes the motors dynamics from the control problem. It is highly nonlinear, heavily coupled and computationally extensive. In contrast, voltage control strategy (VCS) is computationally simple in the form of decentralized

* Corresponding Author's Email: mmfateh@shahroodut.ac.ir (M. M Fateh)

control and free from manipulator's dynamics [11]. The VCS has been already developed for position control of robots driven by the geared permanent magnet dc motors [11]. Motors play a dominant role to control the robot manipulator in VCS. Some control methods in the form of robust voltage control [12], fuzzy control [13], fuzzy task space control [14] time-delay control [15] and adaptive control [16] have used the VCS in position control of robot manipulators driven by permanent magnet dc motors. Applications of control algorithms such as sliding mode control [17], PID control [18], intelligent control [19] and back-stepping control [20] can be extended to the VCS. Literature shows that the above-mentioned common methods are frequently used as speed regulation not for the position control of PMSMs. Moreover, the direct-drive motors are bulky such that handling their dynamics is a challenging problem. In addition, the commonly used TCS for robot manipulators shows the mentioned shortcomings. Considering the problem, causes and solutions, this paper develops the VCS for the first time to the direct-drive robots driven by PMSMs. The paper is organized as follows: section 2 presents modeling of the robotic system. Section 3 develops the VCS. Section 4 analyzes the stability and evaluates the performance of control system. Section 5 gives a comparative study. Section 6 presents the simulation results and finally, section 7 concludes the paper.

2. MODELING

Consider an electrical robot driven directly by PMSMs. The dynamic equation of motion can be expressed as

$$\mathbf{D}(\boldsymbol{\theta})\ddot{\boldsymbol{\theta}} + \mathbf{C}(\boldsymbol{\theta}, \dot{\boldsymbol{\theta}})\dot{\boldsymbol{\theta}} + \mathbf{g}(\boldsymbol{\theta}) = \boldsymbol{\tau} \quad (1)$$

where $\boldsymbol{\theta} \in R^n$ is the vector of joint positions, $\mathbf{D}(\boldsymbol{\theta})$ is the $n \times n$ matrix of manipulator inertia, $\mathbf{C}(\boldsymbol{\theta}, \dot{\boldsymbol{\theta}})\dot{\boldsymbol{\theta}} \in R^n$ is the vector of centrifugal and Coriolis torques, $\mathbf{g}(\boldsymbol{\theta}) \in R^n$ denotes the vector of gravitational torques, and $\boldsymbol{\tau} \in R^n$ is the vector of joint torques. The electric motors provide the joint torques $\boldsymbol{\tau}$ by

$$\mathbf{J}\ddot{\boldsymbol{\theta}} + \mathbf{B}\dot{\boldsymbol{\theta}} + \boldsymbol{\tau} = \boldsymbol{\tau}_m \quad (2)$$

where $\boldsymbol{\tau}_m \in R^n$ is the motors electromagnetic torque vector and \mathbf{J} , and \mathbf{B} , are the $n \times n$ diagonal matrices for inertia and damping of motors, respectively. Note that vectors and matrices are represented in the bold form for clarity. In order to obtain the motor voltages as inputs of the system, consider the electrical equation of the i th PMSM [21] that drive the i th joint as

$$v_{qi} = R_i I_{qi} + L_{qi} \dot{I}_{qi} + P(L_{di} I_{di} + \lambda_{af}) \dot{\theta}_i \quad (3)$$

$$v_{di} = R_i I_{di} + L_{di} \dot{I}_{di} - \dot{\theta}_i P_i L_{qi} I_{qi} \quad (4)$$

where for the i th motor, v_{di} and v_{qi} are the d and q axis voltages, I_{di} and I_{qi} are the d and q axis currents. The coefficient matrices L_{di} and L_{qi} are the d and q axis inductances, R_i is the resistance of stator windings, P_i the number of pole pairs and λ_{af} the amplitude of the flux induced by the permanent magnets of the rotor in the stator phases. Motor torque vector $\boldsymbol{\tau}_m$ as the input for dynamic Equation (2) is produced by the motor currents as

$$\tau_{mi} = 3P_i [\lambda_{af} I_{qi} + (L_{di} - L_{qi}) I_{di} I_{qi}] / 2 \quad (5)$$

The stator voltages of each motor are calculated from v_{di} and v_{qi} of that motor by the inverse park transformation (IPT) as [21]

$$\mathbf{v}_{abc,i} = \mathbf{T}(\theta_i) \mathbf{v}_{qd0,i} \quad (6)$$

$$\mathbf{v}_{abc} = \begin{bmatrix} v_{ai} \\ v_{bi} \\ v_{ci} \end{bmatrix}, \quad \mathbf{v}_{qd0} = \begin{bmatrix} v_{qi} \\ v_{di} \\ v_{0i} \end{bmatrix} \quad \text{and} \quad (7)$$

$$\mathbf{T}(\theta_i) = \begin{bmatrix} \cos(P_i \theta_i) & \sin(P_i \theta_i) & 1 \\ \cos(P_i \theta_i - 2\pi/3) & \sin(P_i \theta_i - 2\pi/3) & 1 \\ \cos(P_i \theta_i + 2\pi/3) & \sin(P_i \theta_i + 2\pi/3) & 1 \end{bmatrix}$$

where v_{0i} is considered to be zero for a balanced system. In order to obtain a state space model for the robotic system driven by PMSMs, we use some mathematics. First, we form matrix equations from Equations (3)-(5) as:

$$\dot{\mathbf{I}}_q = \mathbf{L}_q^{-1} \mathbf{v}_q - \mathbf{L}_q^{-1} \mathbf{R} \mathbf{I}_q - \mathbf{P} \mathbf{L}_q^{-1} \lambda_{af} \dot{\boldsymbol{\theta}} - \mathbf{P} \mathbf{L}_q^{-1} \mathbf{L}_d \boldsymbol{\eta} \quad (8)$$

$$\dot{\mathbf{I}}_d = \mathbf{L}_d^{-1} \mathbf{v}_d + \mathbf{L}_d^{-1} \mathbf{P} \mathbf{L}_q \boldsymbol{\mu} - \mathbf{L}_d^{-1} \mathbf{R} \mathbf{I}_d \quad (9)$$

$$\boldsymbol{\tau}_m = 1.5 \mathbf{P} \lambda_{af} \mathbf{I}_q + 1.5 \mathbf{P} (\mathbf{L}_d - \mathbf{L}_q) \boldsymbol{\xi} \quad (10)$$

where \mathbf{L}_q , \mathbf{L}_d , \mathbf{R} , λ_{af} , and \mathbf{P} are $n \times n$ diagonal matrices formed by the i th element of their diagonal L_{qi} , L_{di} , R_i , λ_{af} , and P_i , respectively. Vectors $\boldsymbol{\eta} \in R^n$, $\boldsymbol{\mu} \in R^n$ and $\boldsymbol{\xi} \in R^n$ are defined through their i th elements as

$$\eta_i = I_{di} \dot{\theta}_i \quad (11)$$

$$\mu_i = \dot{\theta}_i I_{qi} \quad (12)$$

$$\xi_i = I_{di} I_{qi} \quad (13)$$

Substituting Equations (1) and (10) into Equation (2) yields

$$\ddot{\theta} = (\mathbf{D}(\theta) + \mathbf{J})^{-1} \times (1.5P\lambda_{af} \mathbf{I}_q + 1.5P(\mathbf{L}_d - \mathbf{L}_q)\xi - \mathbf{C}(\theta, \dot{\theta})\dot{\theta} - \mathbf{g}(\theta) - \mathbf{B}\dot{\theta}) \quad (14)$$

Using $\mathbf{z}_1 = \theta$, $\mathbf{z}_2 = \dot{\theta}$, $\mathbf{z}_3 = \mathbf{I}_q$ and $\mathbf{z}_4 = \mathbf{I}_d$ as system states, a state space model is then derived from Equations (14), (8) and (9) as

$$\dot{\mathbf{z}} = \mathbf{f}(\mathbf{z}) + \mathbf{b}\mathbf{v} \quad (15)$$

$$\mathbf{f}(\mathbf{z}) = \begin{bmatrix} \mathbf{z}_2 \\ (\mathbf{D}(\mathbf{z}_1) + \mathbf{J})^{-1} (1.5P\lambda_{af}\mathbf{z}_3 + 1.5P(\mathbf{L}_d - \mathbf{L}_q)\xi(\mathbf{z}_3, \mathbf{z}_4) - \mathbf{C}(\mathbf{z}_1, \mathbf{z}_2)\mathbf{z}_2 - \mathbf{g}(\mathbf{z}_1) - \mathbf{B}\mathbf{z}_2) \\ -\mathbf{L}_q^{-1}\mathbf{R}\mathbf{z}_3 - \mathbf{P}\mathbf{L}_q^{-1}\lambda_{af}\mathbf{z}_2 - \mathbf{P}\mathbf{L}_q^{-1}\mathbf{L}_q\eta(\mathbf{z}_1, \mathbf{z}_2) \\ + \mathbf{L}_d^{-1}\mathbf{P}\mathbf{L}_q\mu(\mathbf{z}_2, \mathbf{z}_3) - \mathbf{L}_d^{-1}\mathbf{R}\mathbf{z}_4 \end{bmatrix} \quad (16)$$

$$\mathbf{b} = \begin{bmatrix} \mathbf{0}_{n \times n} & \mathbf{0}_{n \times n} \\ \mathbf{0}_{n \times n} & \mathbf{0}_{n \times n} \\ \mathbf{L}_q^{-1} & \mathbf{0}_{n \times n} \\ \mathbf{0}_{n \times n} & \mathbf{L}_d^{-1} \end{bmatrix}, \mathbf{v} = \begin{bmatrix} \mathbf{0}_{n \times n} & \mathbf{0}_{n \times n} \\ \mathbf{0}_{n \times n} & \mathbf{0}_{n \times n} \\ \mathbf{L}_q^{-1} & \mathbf{0}_{n \times n} \\ \mathbf{0}_{n \times n} & \mathbf{L}_d^{-1} \end{bmatrix}, \mathbf{v} = \begin{bmatrix} \mathbf{v}_q \\ \mathbf{v}_d \end{bmatrix}$$

where voltages of the motors denoted by \mathbf{v}_d and \mathbf{v}_q are considered as the inputs of the robotic system in Equation (15). The state space Equation (15) shows a highly coupled nonlinear large multivariable system. Complexity of the model opens a serious challenge in the literature of robot modeling and control.

3. VOLTAGE CONTROL STRATEGY

VCS opens a new field of research in the control of electrically driven robots. This strategy emphasizes on the control of electric motors of robot for the control of a robot. Its main advantage over the TCS is that the control law becomes free from manipulator model [11]. The VCS has been applied to the electrically driven robots equipped by permanent magnet dc motors [11]. In this Section, we develop the VCS for the direct-drive robots driven by PMSMs. A decentralized voltage control law is proposed as

$$\mathbf{v}_{qi} = R_i \mathbf{I}_{qi} + L_{qi} \dot{\mathbf{I}}_{qi} + u_i P_i (L_{di} \mathbf{I}_{di} + \lambda_{aff}) \quad (17)$$

$$\mathbf{v}_{di} = -\dot{\theta}_i P_i L_{qi} \mathbf{I}_{qi} \quad (18)$$

where u_i is another control input that will be defined next. Applying control laws of Equations (17) and (18) to the PMSM expressed by Equations (3) and (4) gives:

$$u_i = \dot{\theta}_i \quad (19)$$

$$R_i \mathbf{I}_{di} + L_{di} \dot{\mathbf{I}}_{di} = 0 \quad (20)$$

As a result, $\mathbf{I}_{di} \rightarrow 0$ as $t \rightarrow \infty$ since $R_i > 0$ and $L_{di} > 0$. The electrical time constant given by L_{di} / R_i is very short. This follows that $\mathbf{I}_{di} \approx 0$. As a result, the PMSM operates under the maximum torque per ampere [22]. Let us propose the control law u_i for tracking a desired trajectory θ_{di} as

$$u_i = \dot{\theta}_{di} + k_{pi} (\theta_{di} - \theta_i) \quad (21)$$

where k_{pi} is a positive constant. Substituting Equation (21) into Equation (19) yields

$$\dot{e}_i + k_{pi} e_i = 0 \quad (22)$$

where e_i is the tracking error expressed by

$$e_i = \theta_{di} - \theta_i \quad (23)$$

Thus, $e_i \rightarrow 0$ as $t \rightarrow \infty$, if $k_{pi} > 0$. The tracking error will be zero for all $t \geq 0$ if $e_i(0) = 0$. In practice, we can plan the desired trajectory $\theta_{di}(t)$ such that the initial condition is satisfied. Using Equations (17), (18) and (21) presents the control laws in dq frame

$$\mathbf{v}_{qi} = R_i \mathbf{I}_{qi} + L_{qi} \dot{\mathbf{I}}_{qi} + (\dot{\theta}_d + k_{pi} (\theta_d - \theta_i)) P_i (L_{di} \mathbf{I}_{di} + \lambda_{aff}) \quad (24)$$

$$\mathbf{v}_{di} = -\dot{\theta}_i P_i L_{qi} \mathbf{I}_{qi} \quad (25)$$

Applying the IPT Equation (6) to Equations (24) and (25) gives the control law in abc frame

$$\begin{bmatrix} \mathbf{v}_{ai} \\ \mathbf{v}_{bi} \\ \mathbf{v}_{ci} \end{bmatrix} = \mathbf{T}(\theta_i) \times \mathbf{r} \quad (26)$$

$$\mathbf{r} = \begin{bmatrix} R_i \mathbf{I}_{qi} + L_{qi} \dot{\mathbf{I}}_{qi} + (\dot{\theta}_d + k_{pi} (\theta_d - \theta_i)) P_i (L_{di} \mathbf{I}_{di} + \lambda_{aff}) \\ -\dot{\theta}_i P_i L_{qi} \mathbf{I}_{qi} \\ 0 \end{bmatrix}$$

The proposed control law Equation (26) is based on the electrical equations of PMSM i.e. Equations (3) and (4). It is emphasized that the proposed control law is free from robot manipulator dynamic in the form of decentralized structure. This means that each joint is controlled using feedbacks from that joint. According to control law Equation (26), the control system requires feedbacks of joint position θ_i , velocity $\dot{\theta}_i$, currents \mathbf{I}_{qi} and its derivative $\dot{\mathbf{I}}_{qi}$, and \mathbf{I}_{di} . It is verified that none of variables from other joints are given in the control law. The control law has used some constant parameters of each PMSM in control law Equation (25) namely R_i , L_{qi} , L_{di} , P_i and λ_{aff} . One may use the pulse width modulation (PWM) to implement the control law

Equation (25) on the PMSMs using an inverter. The currents of PMSM are measured to calculate I_{qi} and I_{di} using the Park Transformation as follows [21]

$$\begin{bmatrix} I_{qi} \\ I_{di} \\ I_{0i} \end{bmatrix} = \mathbf{T}^{-1}(\theta_i) \begin{bmatrix} I_{ai} \\ I_{bi} \\ I_{ci} \end{bmatrix} \quad (27)$$

4. STABILITY ANALYSIS AND PERFORMANCE EVALUATION

To make the dynamics of tracking error well-defined such that the robot can track the desired trajectory, we make the following assumption.

Assumption 1: *The desired joint trajectory θ_{di} must be smooth in the sense that θ_{di} and its derivatives up to a necessary order are available and all uniformly bounded.*

Smoothness of the desired trajectory can be guaranteed by proper trajectory planning. As a result of applying control law Equations (17), (18) and (21), we obtained Equations (20) and (22) in section 3. Equation (20) implies that

$$I_{di}(t) = I_{di}(0)e^{-\frac{R_i}{L_{di}}t} \quad (28)$$

Hence, $\forall t \geq 0$

$$|I_{di}(t)| \leq |I_{di}(0)| \quad (29)$$

Equation (22) implies that

$$e_i(t) = e_i(0)e^{-k_{pi}t} \quad (30)$$

Using $e_i(t) = \theta_{di}(t) - \theta_i(t)$ results in

$$\theta_i(t) = \theta_{di}(t) - e_i(0)e^{-k_{pi}t} \quad (31)$$

Thus, $\theta_i(t)$ is bounded as

$$|\theta_i(t)| \leq |\theta_{di}(t)| + |e_i(0)| \quad (32)$$

By taking time derivative of Equation (30), we obtain

$$\dot{\theta}_i(t) = \dot{\theta}_{di}(t) + e_i(0)k_{pi}e^{-k_{pi}t} \quad (33)$$

Hence, $\dot{\theta}_i(t)$ is bounded as

$$|\dot{\theta}_i(t)| \leq |\dot{\theta}_{di}(t)| + k_{pi}|e_i(0)| \quad (34)$$

One can calculate $\ddot{\theta}_i(t)$ by taking time derivative of Equation (33) as

$$\ddot{\theta}_i(t) = \ddot{\theta}_{di}(t) - e_i(0)k_{pi}^2e^{-k_{pi}t} \quad (35)$$

Thus, $\ddot{\theta}_i(t)$ is bounded as

$$|\ddot{\theta}_i(t)| \leq |\ddot{\theta}_{di}(t)| + k_{pi}^2|e_i(0)| \quad (36)$$

It can be concluded from Equations (32), (34) and (36) that for each joint $\theta_i(t)$, $\dot{\theta}_i(t)$ and $\ddot{\theta}_i(t)$ are bounded. Extending this result for all joints implies that $\theta_i(t)$, $\dot{\theta}_i(t)$ and $\ddot{\theta}_i(t)$ are bounded. Substituting Equation (1) into Equation (2) yields

$$(\mathbf{J} + \mathbf{D}(\boldsymbol{\theta}))\ddot{\boldsymbol{\theta}} + (\mathbf{B} + \mathbf{C}(\boldsymbol{\theta}, \dot{\boldsymbol{\theta}}))\dot{\boldsymbol{\theta}} + \mathbf{g}(\boldsymbol{\theta}) = \boldsymbol{\tau}_m \quad (37)$$

According to the properties of robot manipulator [23], the inertia matrix $\mathbf{D}(\boldsymbol{\theta})$ and the gravitational forces $\mathbf{g}(\boldsymbol{\theta})$ are bounded. The Coriolis and centripetal matrix $\mathbf{C}(\boldsymbol{\theta}, \dot{\boldsymbol{\theta}})$ are bounded if $\dot{\boldsymbol{\theta}}$ is bounded. Matrices \mathbf{J} and \mathbf{B} are constant. Therefore, $\boldsymbol{\tau}_m$ is bounded as

$$\|\boldsymbol{\tau}_m\| \leq \|\mathbf{J} + \mathbf{D}(\boldsymbol{\theta})\| \cdot \|\ddot{\boldsymbol{\theta}}\| + \|\mathbf{B} + \mathbf{C}(\boldsymbol{\theta}, \dot{\boldsymbol{\theta}})\| \cdot \|\dot{\boldsymbol{\theta}}\| + \|\boldsymbol{\tau}_r(\dot{\boldsymbol{\theta}})\| + \|\mathbf{g}(\boldsymbol{\theta})\| \quad (38)$$

Thus, the torque of i th motor is bounded

$$|\tau_{mi}| \leq \alpha(\boldsymbol{\theta}, \dot{\boldsymbol{\theta}}, \ddot{\boldsymbol{\theta}}) \quad (39)$$

where $\alpha(\boldsymbol{\theta}, \dot{\boldsymbol{\theta}}, \ddot{\boldsymbol{\theta}})$ is a positive scalar. According to Equation (5), if $L_{di} = L_{qi}$, then

$$I_{qi} = (2\tau_{mi} / 3P_i\lambda_{afi}) \quad (40)$$

Thus, I_{qi} is bounded as

$$|I_{qi}| \leq |2 / 3\lambda_{afi}P_i| \cdot |\tau_{mi}| \quad (41)$$

where $2 / 3\lambda_{afi}P_i$ is positive constant and τ_{mi} is bounded as verified in Equation(38). According to Equation (5), if $L_{di} \neq L_{qi}$, then

$$I_{qi} = 2\tau_{mi} / (3P_i[\lambda_{afi} + (L_{di} - L_{qi})I_{di}]) \quad (42)$$

In the RHS of Equation (42), τ_{mi} and I_{di} are bounded and P_i , λ_{afi} , L_{di} and L_{qi} are constant. Thus

$$a \leq 1.5P_i|\lambda_{afi} + (L_{di} - L_{qi})I_{di}| \leq b \quad (43)$$

where a and b are positive scalars. Therefore, I_{qi} is bounded as

$$I_{qi} < |\tau_{mi}| / a \quad (44)$$

According to the reasoning above, for the i th motor $\theta_i(t)$, $\dot{\theta}_i(t)$, I_{qi} and I_{di} for $i = 1, \dots, n$ are bounded. As a result, all system states denoted by $\boldsymbol{\theta}$, $\dot{\boldsymbol{\theta}}$, \mathbf{I}_q and \mathbf{I}_d are bounded.

5. COMPARATIVE STUDY

There would be some shortcoming with the torque control strategy. First, the control law becomes complex due to complexity of manipulator dynamics. In addition, modeling of a direct-drive robot manipulator faces uncertainties including parametric uncertainty, unmodeled dynamics and external disturbances. Then, the control law becomes much complicated to guarantee stability and provide a satisfactory performance. On the other hand, the dynamical terms such as Coriolis and centrifugal torques are highly dominant in the dynamics of a direct-drive robot. Therefore, using robots in high-accuracy and high-speed applications is a challenging problem. We use the model-based control for comparing the VCS with TCS. A torque control law with considering the robot and its actuators based on the model Equation (37) can be suggested as

$$(\mathbf{J} + \mathbf{D}(\boldsymbol{\theta}))(\ddot{\boldsymbol{\theta}}_d + \mathbf{k}_2(\dot{\boldsymbol{\theta}}_d - \dot{\boldsymbol{\theta}}) + \mathbf{k}_1(\boldsymbol{\theta}_d - \boldsymbol{\theta})) + (\mathbf{B} + \mathbf{C}(\boldsymbol{\theta}, \dot{\boldsymbol{\theta}}))\dot{\boldsymbol{\theta}} + \mathbf{g}(\boldsymbol{\theta}) = \boldsymbol{\tau}_m^* \quad (45)$$

where the control design parameters are given by gain diagonal matrices \mathbf{k}_1 and \mathbf{k}_2 . As a result of applying Equation(45) to the model Equation (37), we have

$$\ddot{\boldsymbol{\theta}}_d - \ddot{\boldsymbol{\theta}} + \mathbf{k}_2(\dot{\boldsymbol{\theta}}_d - \dot{\boldsymbol{\theta}}) + \mathbf{k}_1(\boldsymbol{\theta}_d - \boldsymbol{\theta}) = \mathbf{0} \quad (46)$$

Using $\mathbf{k}_1 > 0$ and $\mathbf{k}_2 > 0$, then $\mathbf{x} \rightarrow \mathbf{x}_d$ as $t \rightarrow \infty$ where \mathbf{x} stands for the system states expressed as $\mathbf{x} = [\boldsymbol{\theta} \ \dot{\boldsymbol{\theta}}]$ and $\mathbf{x}_d = [\boldsymbol{\theta}_d \ \dot{\boldsymbol{\theta}}_d]$. Applying control law Equation (45) requires the model of robotic system Equation (37) that is very large, highly nonlinear, heavily coupled and computationally extensive. In addition, the control law Equation (45) requires feedbacks of $\boldsymbol{\theta}$ and $\dot{\boldsymbol{\theta}}$. Then, the actuators of robot are driven so that the proposed torque control is implemented.

The FOC is formed by two inner current control loops and one outer position control loop for position control of robot. The outer loop provides the reference current in q-axis, I_{qi}^* , corresponding to the reference torque, τ_{mi}^* , for one of the inner loops while the other one is a zero reference current in d-axis, I_{di}^* , to achieve the maximum torque per Ampere. The FOC is performed using the PI controllers as follows:

$$v_{qi} = k_{Pqi}(I_{qi}^* - I_{qi}) + k_{Iqi} \int_0^t (I_{qi}^* - I_{qi}) dt \quad (47)$$

where k_{Pqi} and k_{Iqi} are the controller gains, I_{qi}^* is the reference current in q-axis calculated from Equation (5) in non-salient rotor for $L_{di} = L_{qi}$ by

$$I_{qi}^* = \frac{2}{3P_i \lambda_{af}} \tau_{mi}^* \quad (48)$$

where τ_{mi}^* is the i th element of the vector $\boldsymbol{\tau}_m^*$ given by Equation(45). Thus, the vector of \mathbf{I}_q^* is calculated as

$$\mathbf{I}_q^* = \frac{2}{3} \lambda_{af}^{-1} \mathbf{P}^{-1} (\mathbf{J} + \mathbf{D}(\boldsymbol{\theta})) (\ddot{\boldsymbol{\theta}}_d + \mathbf{k}_2(\dot{\boldsymbol{\theta}}_d - \dot{\boldsymbol{\theta}}) + \mathbf{k}_1(\boldsymbol{\theta}_d - \boldsymbol{\theta})) + \frac{2}{3} \lambda_{af}^{-1} \mathbf{P}^{-1} ((\mathbf{B} + \mathbf{C}(\boldsymbol{\theta}, \dot{\boldsymbol{\theta}}))\dot{\boldsymbol{\theta}} + \mathbf{g}(\boldsymbol{\theta})) \quad (49)$$

The model-based control law Equation (49) needs the model of robot. In the literature, the reference current in q-axis \mathbf{I}_q^* was also given as a PD or PID signal on the position error. A reference current in d-axis $I_{di}^* = 0$ is obtained using a PI controller as

$$v_{di} = -k_{Pdi} I_{di} - k_{Idi} \int_0^t I_{di} dt \quad (50)$$

where k_{Pdi} and k_{Idi} are the controller gains.

6. SIMULATON RESULTS

A comparison on the control performances between VCS and TCS implemented by FOC is presented through simulations. All control approaches are applied on a direct-drive three-link articulated robot manipulator driven by PMSMs. Figure 1 shows the initial configuration of the robot manipulator. Denavit-Hartenberg (DH) parameters of the articulated robot are given in Table 1, where the parameters θ_i , d_i , a_i and α_i are called the joint angle, link offset, link length and link twist, respectively. The dynamic parameters of manipulator are given in Table 2, where for the i th link, m_i is the mass, $r_{ci} = [x_{ci} \ y_{ci} \ z_{ci}]^T$ the center of mass expressed in the i th frame, and I_i the inertia tensor expressed in the center of mass frame defined as

$$I_i = \begin{bmatrix} I_{xxi} & I_{xyi} & I_{xzi} \\ I_{xyi} & I_{yyi} & I_{yzi} \\ I_{xzi} & I_{yzi} & I_{zzi} \end{bmatrix} \quad (51)$$

The parameters of motors are given in Table 3. The controllers are selected with the same structure for three joints, but their gains might be different. The desired position for $i = 1, 2, 3$ is given the same form of

$$\theta_{di} = 3t^2 - 2t^3 \quad (52)$$

where the operating time is given 1 sec. The desired trajectory starts from zero and after 1 second reaches 1 rad . The goal of control system is to track the desired trajectory expressed by Equation (52) from the initial configuration of the robot.

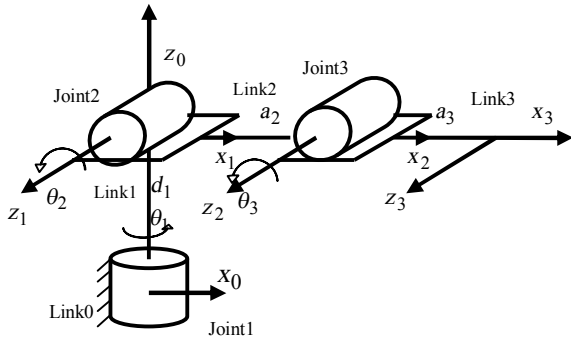


Figure 1. Articulated three-link robot manipulator

TABLE 1. The DH parameters

Link	θ	d	a	α
1	θ_1	$d_1 = 0.280$	0	$\pi / 2$
2	θ_2	0	$a_2 = 0.760$	0
3	θ_3	0	$a_3 = 0.930$	0

TABLE 2. The parameters of articulated robot

i	x_i	y_i	z_i	m_i	I_{xxi}	I_{yyi}	I_{zzi}
1	0	-0.22	0	19	0.34	0.36	0.31
2	-0.51	0	0	18.18	0.18	1.32	1.31
3	-0.67	0	0	10.99	0.07	0.92	0.93

$I_{xyi} = I_{xzi} = I_{yzi} = 0$

TABLE 3. The specifications of PMSMs

L_d	L_q	λ_{af}	R	J	B	P
0.00095	0.00095	10	1	0.008	0.001147	4

TABLE 4. The gains of controllers in FOC

	k_{1i}	k_{2i}	k_{pqi}	k_{Iqi}	k_{Pdi}	k_{Idi}
Cont.1	1000	100	50	50	10	10
Cont.2	100	10	50	50	10	10
Cont.3	100	1000	50	50	10	10

Simulation 1: We apply VCS on the control system using control law Equations (16) and (17). The controllers are selected the same with $k_{pi} = 100$ for $i = 1, 2, 3$. The performance of VCS is shown in Figure 2 where the maximum tracking error for joint 2 is about $5.33 \times 10^{-5} \text{ rad}$. The tracking error is really ignorable while the robot starts under a high load as shown in Figure 1.

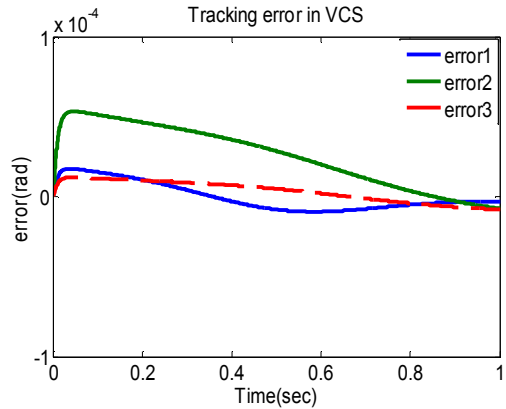


Figure 2. Tracking performance of the VCS

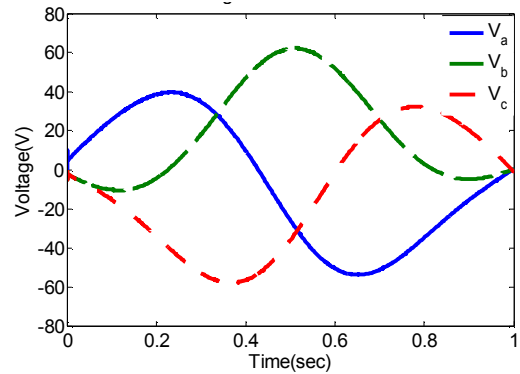


Figure 3. The control efforts of the controller 2

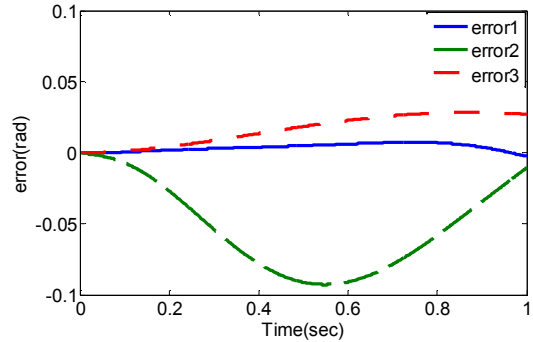


Figure 4. Tracking performance of FOC

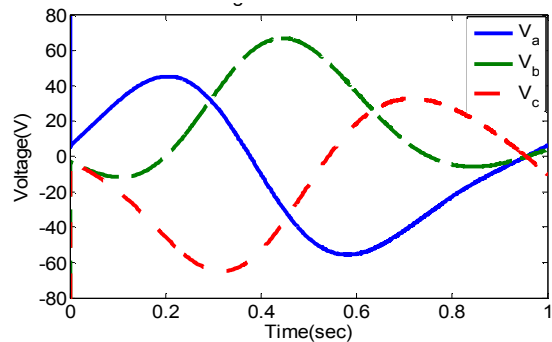


Figure 5. The control efforts of controller 2

It is worthy to note that the joint 2 has the most load torque, thus we have shown its performance. The control efforts behave smoothly as shown for the controller 2 in Figure 3.

Simulation 2: We apply the FOC on the control system using control laws Equations (45), (47) and (49). The gains of controllers are given in Table 4.

The performance of FOC is shown in Figure 4 where the maximum tracking error for joint 2 is about 0.0284 rad . The tracking error is not as small as that the one for the VCS. The maximum tracking error for joint 2 is about 532 times larger than its value in the VCS but is similar to its value in the modified DTC. The control efforts rapidly increase to a high value, but reduce with oscillations as shown for the controller 2 in Figure 5. After a while the motor voltages behave similar to ones in the VCS.

7. CONCLUSION

The tracking control of the direct-drive robot manipulators driven by PMSMs has been studied in this paper. The robotic control system commonly uses the torque control strategy that is highly nonlinear, heavily coupled and extensively computational due to complexity manipulator dynamics. One may use the FOC to perform this strategy in position control of robots. The problem is that the FOC is usually employed for speed regulation of the PMSMs. In addition, the control of a direct-drive robot manipulator is relatively more difficult than the geared-drive robot manipulator due to the dynamical terms. Considering these problems, this paper has presented a novel control approach using the VCS. Results confirm that VCS is superior to TCS due to being free from manipulator dynamics. The proposed control approach can be used to perform the high-speed tasks with high-accuracy.

8. REFERENCES

1. Foo, G. and Rahman, M., "Sensorless direct torque and flux-controlled ipm synchronous motor drive at very low speed without signal injection", *Industrial Electronics, IEEE Transactions on*, Vol. 57, No. 1, (2010), 395-403.
2. Corradini, M.L., Ippoliti, G., Longhi, S. and Orlando, G., "A quasi-sliding mode approach for robust control and speed estimation of pm synchronous motors", *Industrial Electronics, IEEE Transactions on*, Vol. 59, No. 2, (2012), 1096-1104.
3. Kazmierkowski, M.P., Franquelo, L.G., Rodriguez, J., Perez, M.A. and Leon, J.I., "High-performance motor drives", *Industrial Electronics Magazine, IEEE*, Vol. 5, No. 3, (2011), 6-26.
4. Blaschke, F., "The principle of field-orientation as applied to the trans vector closed loop control system for rotating-field machines", *Siemens Review*, Vol. 34, No., (1972), 217-220.
5. Zhong, L., Rahman, M.F., Hu, W.Y. and Lim, K., "Analysis of direct torque control in permanent magnet synchronous motor drives", *Power Electronics, IEEE Transactions on*, Vol. 12, No. 3, (1997), 528-536.
6. Rahman, M.F., Zhong, L. and Lim, K.W., "A direct torque-controlled interior permanent magnet synchronous motor drive incorporating field weakening", *Industry Applications, IEEE Transactions on*, Vol. 34, No. 6, (1998), 1246-1253.
7. Zhong, L., Rahman, M.F., Hu, W., Lim, K. and Rahman, M., "A direct torque controller for permanent magnet synchronous motor drives", *Energy Conversion, IEEE Transactions on*, Vol. 14, No. 3, (1999), 637-642.
8. Pacas, M., "Sensorless drives in industrial applications", *Industrial Electronics Magazine, IEEE*, Vol. 5, No. 2, (2011), 16-23.
9. Lin, F.-J. and Lin, Y.-S., "A robust pm synchronous motor drive with adaptive uncertainty observer", *Energy Conversion, IEEE Transactions on*, Vol. 14, No. 4, (1999), 989-995.
10. Rashed, M., MacConnell, P.F., Stronach, A.F. and Acarnley, P., "Sensorless indirect-rotor-field-orientation speed control of a permanent-magnet synchronous motor with stator-resistance estimation", *Industrial Electronics, IEEE Transactions on*, Vol. 54, No. 3, (2007), 1664-1675.
11. Fateh, M.M., "On the voltage-based control of robot manipulators", *International Journal of Control, Automation, and Systems*, Vol. 6, No. 5, (2008), 702-712.
12. Fateh, M.M., "Robust voltage control of electrical manipulators in task-space", *International Journal of Innovative Computing, Information and Control*, Vol. 6, No. 6, (2010), 2691-2700.
13. Fateh, M.M., "Robust fuzzy control of electrical manipulators", *Journal of Intelligent & Robotic Systems*, Vol. 60, No. 3-4, (2010), 415-434.
14. Fateh, M.M., "Fuzzy task-space control of a welding robot", *International Journal of Robotics & Automation*, Vol. 25, No. 4, (2010), 372.
15. Fateh, M.M., "Robust control of flexible-joint robots using voltage control strategy", *Nonlinear Dynamics*, Vol. 67, No. 2, (2012), 1525-1537.
16. Fateh, M.M., "Nonlinear control of electrical flexible-joint robots", *Nonlinear Dynamics*, Vol. 67, No. 4, (2012), 2549-2559.
17. Rakhtala, S., Ranjbar, A. and Ghaderi, R., "Systematic approach to design a finite time convergent differentiator in second order sliding mode controller", *International Journal of Engineering-Transactions B: Applications*, Vol. 26, No. 11, (2013), 1357.
18. Babu, R., Samuel, R., Deepa, S. and Jothivel, S., "A closed loop control of quadratic boost converter using pid-controller", *International Journal of Engineering, Transactions B: Applications*, Vol. 27, No. 11, (2014).
19. Garmsiri, N., Najafi, F. and Saadat, M., "A new intelligent approach to patient-cooperative control of rehabilitation robots", *International Journal of Engineering-Transactions C: Aspects*, Vol. 27, No. 3, (2013), 467.
20. Gholipour, R., Khosravi, A. and Mojjallali, H., "Suppression of chaotic behavior in duffing-holmes system using back-stepping controller optimized by unified particle swarm optimization algorithm", *International Journal of Engineering-Transactions B: Applications*, Vol. 26, No. 11, (2013), 1299.
21. Krause, P.C., Wasynczuk, O., Sudhoff, S.D. and Pekarek, S., "Analysis of electric machinery and drive systems, John Wiley & Sons, Vol. 75, (2013).
22. Bose, B.K., Power electronics and variable frequency drives., IEEE press Piscataway, New Jersey.(1997)
23. Qu, Z. and Dawson, D.M., "Robust tracking control of robot manipulators, IEEE press, (1995).

Voltage Control Strategy for Direct-drive Robots Driven by Permanent Magnet Synchronous Motors

M. M. Fateh, M. Sadeghijaleh

Department of Electrical and Robotic Engineering, Shahrood University of Technology, Iran

PAPER INFO

چکیده

Paper history:

Received 15 August 2014

Received in revised form 11 October 2014

Accepted in 18 December 2014

Keywords:

Direct-Drive Robot

Permanent Magnet Synchronous Motor

Torque Control Strategy

Voltage Control Strategy

راهبرد کنترل گشتاور، راهبردی مرسوم در کنترل بازوهای رباتیکاست. با وجود این، پیچیدگی‌های دینامیک بازوی رباتیک موجب پیچیدگی کنترل گشتاور شده است. به علاوه، کنترل موقعیت موتورهای سنکرون مغناطیس دائم دشوار است؛ در نتیجه ردگیری ربات‌های رانده شده توسط موتورهای سنکرون مغناطیس دائم چالش محسوب می‌شود. این مقاله روش کنترلی جدید ساده و مستقل از مدل ربات به منظور کنترل ردگیری ربات‌های رانده شده توسط محرکه الکتریکی ارائه می‌کند. نوآوری مقاله توسعه استراتژی کنترل ولتاژ برای ربات‌های رانده شده توسط موتورهای سنکرون مغناطیس دائم بدون چرخ‌دنده است. علاوه بر این، یک مدل فضای حالت برای کل سیستم رباتیک شامل بازوی ربات و موتورهای سنکرون مغناطیس دائم بدون چرخ-دنده ارائه می‌شود. سپس، درستی روش پیشنهادی با تحلیل پایداری اثبات می‌شود. مقایسه‌ها و شبیه‌سازی برتری راهبرد کنترل ولتاژ بر راهبرد کنترل گشتاور نشان می‌دهد.

doi: 10.5829/idosi.ije.2015.28.05b.09